

Event multiplicity, transverse momentum and energy dependence of charged particle production, and system thermodynamics in pp collisions at the Large Hadron Collider

Rutuparna Rath^a, Arvind Khuntia^{b*}, Raghunath Sahoo^{a†}, and Jean Cleymans^{c‡}

^a*Discipline of Physics, School of Basic Sciences,
Indian Institute of Technology Indore, Simrol, Indore 453552, India*

^b*The H. Niewodniczanski Institute of Nuclear Physics,
Polish Academy of Sciences, PL-31342 Krakow, Poland and*

^c*UCT - CERN Research Centre, Physics Department,
University of Cape Town, Rondebosch - 7701, South Africa*

(Dated: September 13, 2022)

In the present work, we study the recent collision energy and multiplicity dependence of the charged particle transverse momentum spectra as measured by the ALICE collaboration in pp collisions at $\sqrt{s} = 5.02$ and 13 TeV using the non-extensive Tsallis distribution and the Boltzmann-Gibbs Blast Wave (BGBW) model. A thermodynamically consistent form of the Tsallis distribution is used to extract the kinetic freeze-out parameters from the transverse momentum spectra of charged particles at mid-rapidity. In addition, a comprehensive study of fitting the range dependence of transverse momentum spectra on the freeze-out parameters is done using Tsallis statistics. The applicability of BGBW model is verified by fitting the transverse momentum spectra of the bulk part (~ 2.5 GeV/ c) for both 5.02 and 13 TeV energies and also in different multiplicity classes. The radial flow, $\langle \beta \rangle$ is almost independent of collision energy and multiplicity whereas the behavior of kinetic freeze-out temperature significantly depends on multiplicity classes. It is found that the Tsallis distribution generally leads to a better description than the Blast Wave model.

PACS numbers:

I. INTRODUCTION

Transverse momentum spectra of final state particles produced in high energy collisions provide important information about the dynamics of high energy collisions. Previously pp collisions at the Relativistic Heavy-ion Collider (RHIC) and the Large Hadron Collider (LHC) provided a baseline for the understanding of particle production in heavy-ion collisions. However, recent results on the multiplicity dependence in pp collisions at $\sqrt{s} = 7$ TeV, which showed similar results at high multiplicities to those obtained in heavy-ion collisions [1] have led to question whether or not this is relevant. Strangeness enhancement as one of the possible signatures for the formation of a QGP droplet in pp collisions has led to new challenges to understand the particle production mechanism in high multiplicity pp collisions. The multi-partonic interactions in high multiplicity pp collisions lead to the formation of more number of final state hadrons, which might favor a thermalisation in the system in such collisions. Thus such a complicated system can be explained by statistical models with few parameters. The study of transverse momentum spectra of final state particles provides informations about the kinetic freeze-out processes in high energy collisions. The use of Tsallis non-extensive statistics leads to a power law distribution with excellent fits of the transverse momentum spectra of charged par-

ticles and identified particles in high energy collisions up to very high values of p_T [2–15]. This description can be understood as containing temperature fluctuations in the Boltzmann-Gibbs sense either on an event-by-event basis or within the same event [16]. This fluctuation in the temperature is directly related to the non-extensive parameter q [17] and tells us about the departure of the system from an equilibrium state. In the present analysis, we have explicitly checked the variation of the non-extensive parameter q and the Tsallis temperature with the fitting range involved for the transverse momentum spectra of charged particle produced in high energy pp collisions at LHC energies [18].

As an alternative, perhaps more standard description, we have used a blast-wave model based on collective flow in small systems. One way to extract information about the radial flow is by studying the transverse momentum spectra of charged particles with the use of the BGBW model, which incorporates the radial flow into the Boltzmann-Gibbs distribution function. The BGBW model is quite good in explaining the bulk part of the system, however it fails at low- p_T which could possibly be due to the decays of hadronic resonances. In this paper we extract the information about the kinetic freeze-out temperature and radial flow from the charged particle p_T -distributions at the highest LHC energies as a function of multiplicity. We compare the Tsallis non-extensive statistics and the BGBW model in detail in the next section.

The paper is organized as follows. In Sec. II, we briefly recall the details of the thermodynamically consistent Tsallis distribution function and also the BGBW model used to describe the charged particle p_T -spectra

*e-mail: Arvind.Khuntia@cern.ch

†Corresponding author: Raghunath.Sahoo@cern.ch

‡e-mails: jean.cleymans@gmail.com; jean.cleymans@uct.ac.za

at mid-rapidity produced in pp collisions at $\sqrt{s} = 5.02$ and 13 TeV. The results obtained using the Tsallis non-extensive statistics and BGBW model are discussed as a function of charged particle multiplicity and collision energy in Sec. III. Finally, in Sec. IV, we present the summary of our results.

II. METHODOLOGY

A. Non-extensive Tsallis statistics

The Tsallis non-extensive distribution function accounts for the power-law contribution at high- p_T and this could be understood as empirically taking of QCD contributions. It is given by:

$$f(E) \equiv \exp_q \left(-\frac{E - \mu}{T} \right), \quad (1)$$

where $E = \sqrt{p^2 + m^2}$, is the energy and μ is the chemical potential of the system and the $\exp_q(x)$ has the following form:

$$\exp_q(x) \equiv \begin{cases} [1 + (q-1)x]^{1/(q-1)} & \text{if } x > 0 \\ [1 + (1-q)x]^{1/(1-q)} & \text{if } x \leq 0 \end{cases} \quad (2)$$

in the limit, $q \rightarrow 1$, Eq. (2) reduces to the standard exponential function:

$$\lim_{q \rightarrow 1} \exp_q(x) \rightarrow \exp(x).$$

The expressions of the relevant thermodynamic quantities like entropy, S , energy density, $\epsilon (= E/V)$, pressure, P , and particle number, N , are given below. Note that an addition power of q in Eq. (1) is necessary to make Tsallis statistics thermodynamically consistent [2, 3, 5].

$$\begin{aligned} S &= -gV \int \frac{d^3p}{(2\pi)^3} [f^q \ln_q f - f], \\ \epsilon &= g \int \frac{d^3p}{(2\pi)^3} E f^q, \\ P &= g \int \frac{d^3p}{(2\pi)^3} \frac{p^2}{3E} f^q, \\ N &= gV \int \frac{d^3p}{(2\pi)^3} f^q, \end{aligned} \quad (3)$$

with g being the degeneracy factor and V is the (Tsallis) freeze-out volume.

The yield can be written in the following form, as deduced from Eq. (3):

$$E \frac{d^3N}{dp^3} = gVE \frac{1}{(2\pi)^3} \left[1 + (q-1) \frac{E - \mu}{T} \right]^{-\frac{q}{q-1}}, \quad (4)$$

and can be written in the form of rapidity, y , transverse mass, m_T , and transverse momentum, p_T :

$$\begin{aligned} \left. \frac{d^2N}{dp_T dy} \right|_{y=0} &= gV \frac{p_T m_T \cosh y}{(2\pi)^2} \\ &\left[1 + (q-1) \frac{m_T \cosh y - \mu}{T} \right]^{-\frac{q}{q-1}}. \end{aligned} \quad (5)$$

At LHC energies, assuming the chemical potential, $\mu \simeq 0$ and at mid-rapidity i.e, $y = 0$ this reduces to:

$$\begin{aligned} \left. \frac{d^2N}{dp_T dy} \right|_{y=0} &= gV \frac{p_T m_T}{(2\pi)^2} \\ &\left[1 + (q-1) \frac{m_T}{T} \right]^{-\frac{q}{q-1}}. \end{aligned} \quad (6)$$

Furthermore, integration over the transverse momentum of Eq. (6) leads to [19]:

$$\begin{aligned} \left. \frac{dN}{dy} \right|_{y=0} &= \frac{gV}{(2\pi)^2} \int_0^\infty p_T dp_T m_T \left[1 + (q-1) \frac{m_T}{T} \right]^{-\frac{q}{q-1}} \\ &= \frac{gVT}{(2\pi)^2} \left[\frac{(2-q)m^2 + 2mT + 2T^2}{(2-q)(3-2q)} \right] \\ &\left[1 + (q-1) \frac{m}{T} \right]^{-\frac{1}{q-1}}. \end{aligned} \quad (7)$$

This makes it possible to eliminate the volume V in favor of the yield at mid-rapidity dN/dy . Now we can write the invariant yield for the charged particles with assumption that it is dominated by the production of π , K and p and in this case we have considered the weight factor 0.8, 0.12 and 0.08 for π , K and p , respectively:

$$\begin{aligned} \left. \frac{d^2N_{ch}}{dp_T dy} \right|_{y=0} &= A \sum_{i=\pi, K, p} w_i \frac{m_T}{T} p_T \\ &\left[\frac{(2-q)m_i^2 + 2m_i T + 2T^2}{(2-q)(3-2q)} \right]^{-1} \\ &\left[1 + (q-1) \frac{m_i}{T} \right]^{-\frac{1}{1-q}} \\ &\left[1 + (q-1) \frac{m_T}{T} \right]^{-\frac{q}{q-1}}, \end{aligned} \quad (8)$$

here A is the charged particle yield at mid-rapidity, q is the non-extensive parameter and T is the Tsallis temperature of the system.

B. Boltzmann-Gibbs Blast Wave (BGBW) Model

As an alternative description, we compare the fits using the Tsallis distribution with the BGBW model. The expression for the invariant yield in the framework of BGBW, where particles decouple from the system at a temperature T_{kin} is given as follows [20]:

$$E \frac{d^3 N}{dp^3} = D \int d^3 \sigma_\mu p^\mu \exp\left(-\frac{p^\mu u_\mu}{T}\right), \quad (9)$$

where $p^\mu = (m_T \cosh y, p_T \cos \phi, p_T \sin \phi, m_T \sinh y)$, is the particle four-momentum and the four-velocity $u^\mu = \cosh \rho (\cosh \eta, \tanh \rho \cos \phi_r, \tanh \rho \sin \phi_r, \sinh \eta)$.

Again, the kinetic freeze-out surface is parametrised as,

$$d^3 \sigma_\mu = (\cosh \eta, 0, 0, -\sinh \eta) \tau r dr d\eta d\phi_r, \quad (10)$$

where, η is the space-time rapidity. Now assuming Bjorken correlation in rapidity i.e, $y = \eta$ [21],

$$\left. \frac{d^2 N}{dp_T dy} \right|_{y=0} = D \int_0^{R_0} r dr K_1\left(\frac{m_T \cosh \rho}{T_{kin}}\right) I_0\left(\frac{p_T \sinh \rho}{T_{kin}}\right), \quad (11)$$

here D is the normalization constant and $m_T = \sqrt{p_T^2 + m^2}$ is the transverse mass while K_1 and I_0 are the modified Bessel functions, $\rho = \tanh^{-1} \beta$, with $\beta = \beta_s \left(r/R_0\right)^n$, [20, 22, 23] is the velocity of the transverse expansion. Again β_s is the maximum surface velocity and the exponent n describes the evolution of the flow velocity from any arbitrary r to R ($r < R$), with R being the maximum radius at the kinetic freeze-out surface.

Now, the average of the transverse velocity can be evaluated as:

$$\langle \beta \rangle = \frac{\int \beta_s \xi^n \xi d\xi}{\int \xi d\xi} = \left(\frac{2}{2+n}\right) \beta_s, \quad (12)$$

where $\xi = r/R_0$.

For the charged particle transverse momentum distribution in case of BGBW we have considered the linear flow profile ($n = 1$) and also weight factors 0.8, 0.12 and 0.08 are considered for π , K and p respectively, which is the same procedure as used for the Tsallis distribution.

III. RESULTS AND DISCUSSION

A. Non-extensive statistics

The transverse momentum spectra (p_T) of charged particles in pp collisions at $\sqrt{s} = 5.02$ and 13 TeV have been fitted with the Tsallis non-extensive distribution as shown in Fig. 1 and 2 [18]. The fitting is also performed for different multiplicity classes as given in Table I and II, at both energies using non-extensive statistics. The charged particle production might vary in different p_T regions and the p_T -differential deviation of the fitting function from the charged particle transverse momentum spectra are shown in the bottom panel.

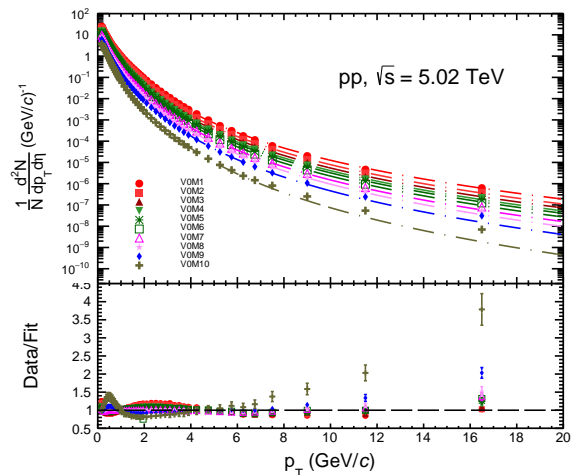


FIG. 1: (Color online) Charged particle spectra fit with Tsallis distribution function for pp collisions at $\sqrt{s} = 5.02$ TeV [18].

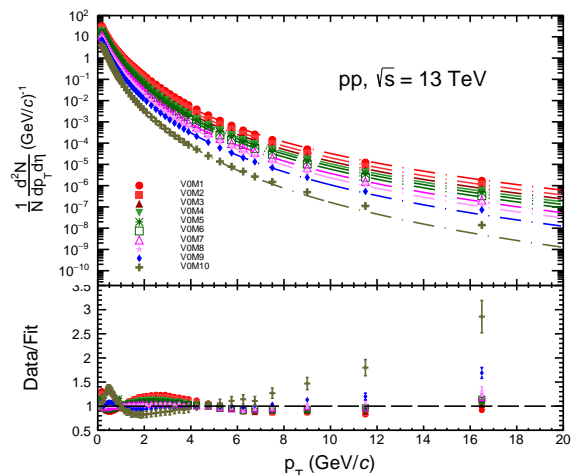


FIG. 2: (Color online) Charged particle spectra fit with Tsallis distribution function for pp collisions at $\sqrt{s} = 13$ TeV [18].

From the ratio between the experimental data points and the fit function, it is observed that the non-extensive statistics provides a good description of the charged particle transverse momentum spectra for the complete p_T region. However, in the highest transverse momentum region the fitting is better for the higher multiplicity classes as compared to the lower multiplicity classes.

The extracted non-extensive parameter, q , shown in Fig. 3 increases with multiplicity classes and remains almost constant above $\sim |dN_{ch}/d\eta|_{|\eta| < 0.8} > 15$. The non-extensive parameter is higher for the 13 TeV and this can be understood as the contributions from the hard scatterings in pp at $\sqrt{s} = 13$ TeV is larger than at 5.02

TABLE I: Number of mean charged particle multiplicity density corresponding to different multiplicity classes in pp collisions at $\sqrt{s} = 5.02$ TeV [18].

Class name	V0M1	V0M2	V0M3	V0M4	V0M5	V0M6	V0M7	V0M8	V0M9	V0M10
$\langle \frac{dN_{ch}}{d\eta} \rangle$	19.2 ± 0.9	15.1 ± 0.7	12.4 ± 0.5	10.7 ± 0.5	9.47 ± 0.47	8.04 ± 0.42	6.56 ± 0.37	5.39 ± 0.32	4.05 ± 0.27	2.27 ± 0.27

TABLE II: Number of mean charged particle multiplicity density corresponding to different multiplicity classes in pp collisions at $\sqrt{s} = 13$ TeV [18].

Class name	V0M1	V0M2	V0M3	V0M4	V0M5	V0M6	V0M7	V0M8	V0M9	V0M10
$\langle \frac{dN_{ch}}{d\eta} \rangle$	26.6 ± 1.1	20.5 ± 0.8	16.7 ± 0.7	14.3 ± 0.6	12.6 ± 0.5	10.6 ± 0.5	8.46 ± 0.40	6.82 ± 0.34	4.94 ± 0.28	2.54 ± 0.26

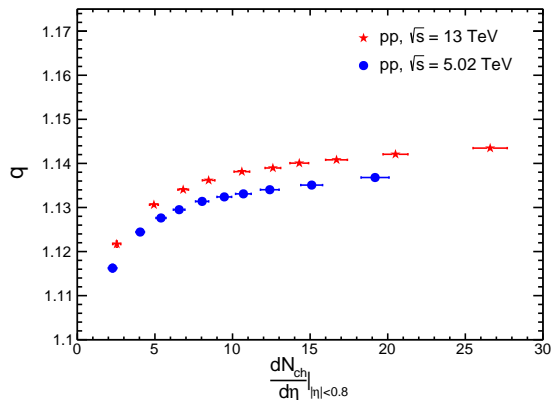


FIG. 3: (Color online) Non-extensive parameter as a function of charged particle multiplicity and collision energy.

TeV.

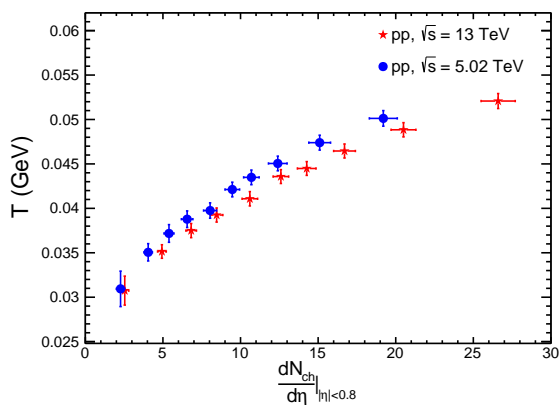


FIG. 4: (Color online) Tsallis temperature as a function of charged particle multiplicity and collision energy.

Furthermore, similar behavior is observed for the Tsallis temperature, T and this shows a significant dependence on the multiplicity class as shown in Fig. 4. There is also a clear energy dependence of T and it is higher for 5.02 TeV.

A comprehensive study of the extracted parameter dependence on the fitting range of charged particle transverse momentum spectra is performed in this work. Here, we have considered the highest and lowest charged particle multiplicity classes for both the energies. The maximum value of transverse momentum in the fitting ranges from 1.2 to 20 GeV/c and the extracted parameters are drawn and filled at the higher edge of the p_T as shown in Fig. 5, 6 and 7. The goodness of the fit i.e., χ^2/ndf as a function of fitting range is shown in Fig. 5.

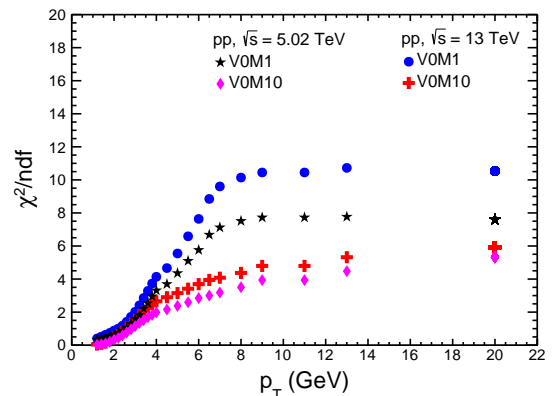


FIG. 5: (Color online) χ^2/ndf obtained by varying the fitting ranges in the p_T -spectra for pp at $\sqrt{s} = 5.02$ and 13 TeV for V0M1 and V0M10 classes.

The non-extensive parameters q have been extracted by varying the fitting ranges and are shown in Fig. 6, for both V0M1 (high multiplicity) and V0M10 (low multiplicity) multiplicity classes. The non-extensive parameter, q shows a reverse trend for both highest and lowest multiplicity classes as a function of fitting range. The charged particle production at high- p_T has power-law contributions and this increases with multiplicity classes [18].

This is evident from the fact that the p_T spectra of the charged particles evolve with multiplicity class and the differential ratios of transverse momentum spectra with respect to minimum bias shows hardening of p_T -spectra with multiplicity classes [18]. For the V0M1 class, the addition of high- p_T charged particles increases

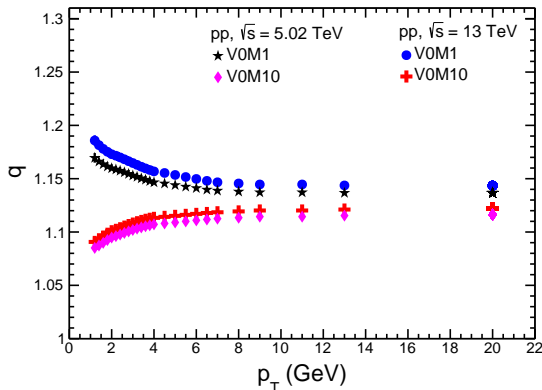


FIG. 6: (Color online) Non-extensive parameter obtained by varying the fitting ranges in the p_T -spectra for pp at $\sqrt{s} = 5.02$ and 13 TeV for V0M1 and V0M10 classes.

the power-law contributions, which correspond to hard pQCD processes. However, this leads to the lowering the values of q with extending the fitting range in the non-extensive statistics for the highest multiplicity class, which shows a saturation behavior beyond $p_T \sim 8$ GeV/c. Contrary to the highest multiplicity class (V0M1), for the V0M10 class (lowest multiplicity class), extending the fitting range has less power-law contribution compared to V0M1. This could be seen from the absolute values of the q -parameter for both the classes. For V0M10, q increases with the fitting range in the non-extensive statistics approaching a saturation behavior beyond $p_T \sim 8$ GeV/c. The non-extensive parameter, q doesn't depend on the fitting range above 8 GeV/c for both V0M1 and V0M10 classes.

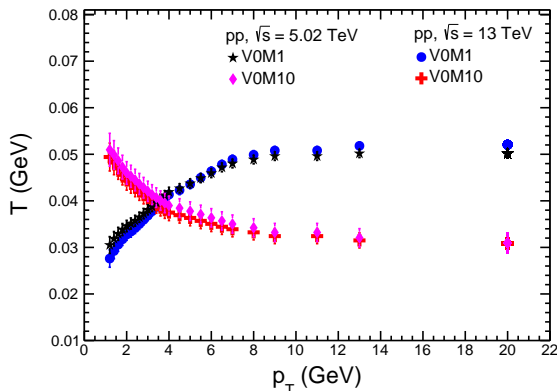


FIG. 7: (Color online) Tsallis temperature parameter obtained by varying the fitting ranges in the p_T -spectra for pp at $\sqrt{s} = 5.02$ and 13 TeV for V0M1 and V0M10 classes.

Similarly the Tsallis temperature, T , evolves with fitting range and has opposite behavior for V0M1 and V0M10 classes as shown in Fig. 7. The Tsallis tem-

perature, T , increases with fitting range for V0M1 class, whereas the trend for V0M10 class is reverse and it decreases with the fitting range. Furthermore, T is almost independent of the fitting range for both 5.02 and 13 TeV beyond $p_T \sim 8$ GeV/c. As it appears, $p_T \sim 8$ GeV/c seems to be a threshold for a different behavior in particle production.

B. BGBW model

In this section, we analyse the bulk part (up to $\simeq 2.5$ GeV/c) of the transverse momentum spectra of the charged particle using a BGBW model and characterize the system at the kinetic freeze-out with transverse collective flow velocity (β) and the kinetic freeze-out temperature (T_{kin}). Fig. 8 and 9, show the fit to the charged particle transverse momentum spectra in pp collisions at $\sqrt{s} = 5.02$ and 13 TeV for different multiplicity classes. The bottom panel shows the ratios between the experimental data points and the BGBW function and the goodness of fit i.e. χ^2/ndf is shown by Fig. 10. The χ^2/ndf is large and the contributions mostly come from the low- p_T region.

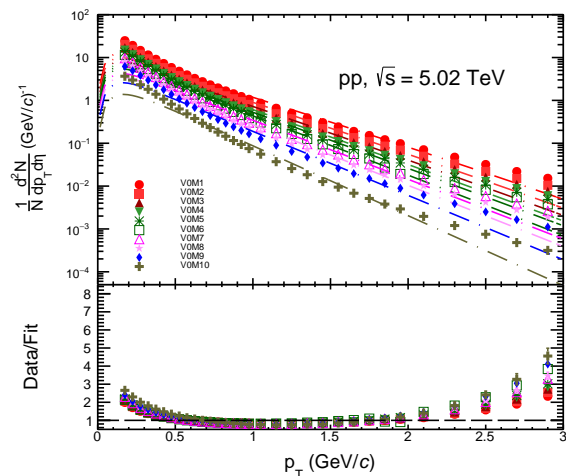


FIG. 8: (Color online) Charged particle spectra fit with BGBW function for pp collisions at $\sqrt{s} = 5.02$ TeV [18].

The BGBW model clearly underestimates the charged particle transverse momentum spectra at low- p_T and thus the deviation of the BGBW function from the experimental data points at low- p_T arises which is possibly due to the contributions from resonance decays. The BGBW fit is better for the higher charged particle multiplicity classes as compared to the lower multiplicity classes.

The kinetic freeze-out parameters, the radial flow (β) and kinetic freeze-out temperature T_{kin} are extracted using the BGBW model for various multiplicity classes and are shown in Fig. 11 and 12. The radial flow (β) is

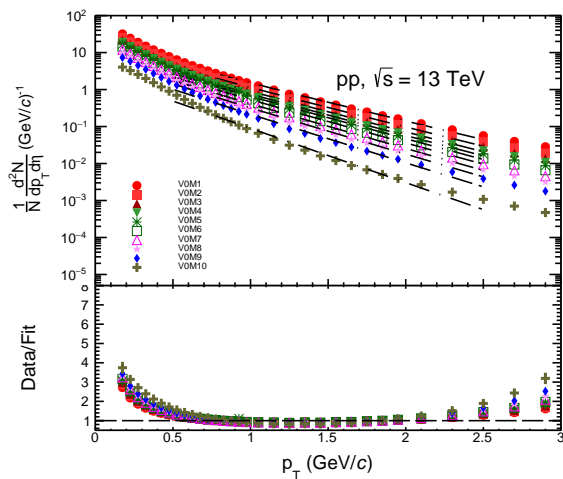


FIG. 9: (Color online) Charged particle spectra fit with BGBW function for pp collisions at $\sqrt{s} = 13$ TeV [18].

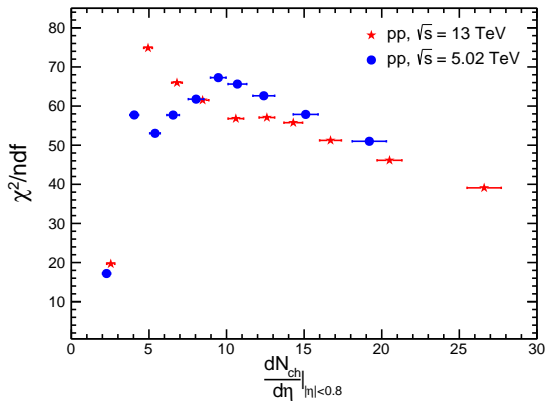


FIG. 10: (Color online) The values of χ^2 divided by the number of degrees of freedom as a function of the charged particle multiplicity and collision energy for the BGBW analysis.

almost independent of the collision energy and multiplicity classes, however the fittings are worst for the lower multiplicity classes in case of BGBW model. The kinetic freeze-out temperature, T_{kin} however shows a clear dependence on the multiplicity class. Furthermore, T_{kin} is higher for the lower multiplicity classes for both the collision energies and it decreases with a larger number of charged particles in the system.

IV. SUMMARY

In the present work, we have analyzed the charged particle transverse momentum spectra in pp collisions at $\sqrt{s} = 5.02$ and 13 TeV energies using the thermodynamically consistent Tsallis non-extensive statistics and, as

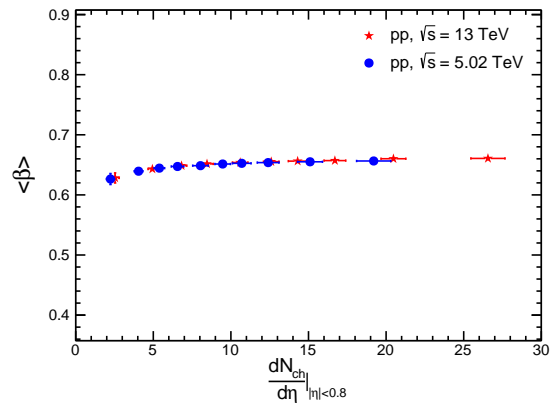


FIG. 11: (Color online) Radial flow velocity parameter as a function of charged particle multiplicity and collision energy.

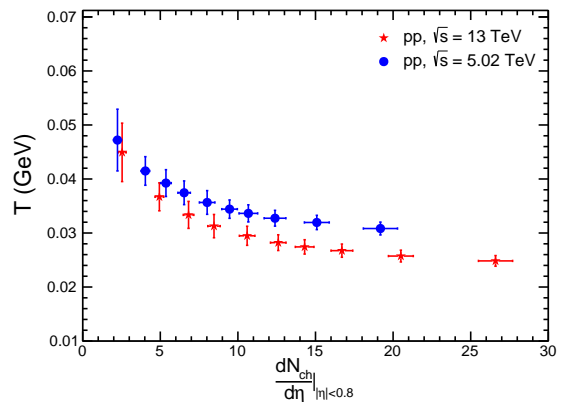


FIG. 12: (Color online) Temperature as a function of charged particle multiplicity and collision energy.

a comparison, the BGBW model. In both the cases, a weight factor of 0.8, 0.12 and 0.08 have been considered for π , K and p respectively due to the fact that charged particles are mostly dominated by these three particles. A consistent picture of the extracted parameters emerges from the comparison to the experimental data as a function of charged particle multiplicity and collision energy and the important results are summarized below:

- The non-extensive Tsallis distributions leads to an excellent description of experimental data for the complete transverse momentum range in various multiplicity classes and collision energies.
- The deviation of the non-extensive parameter, q from unity tells about the departure of the system from thermodynamic equilibrium and it increases with multiplicity classes and remains almost constant above $\sim |dN_{ch}/d\eta|_{|\eta|<0.8} > 15$.
- In line with other observations like multipartonic interactions dominantly contributing to the final

state particle production [24], and the observation of a thermodynamic limit for statistical ensembles to converge [25], final state charged particle multiplicity $\sim |dN_{ch}/d\eta|_{|\eta|<0.8} > 15$ appears to be a threshold number in particle production in hadronic collisions at the TeV energies.

- Higher values of the non-extensive parameter is observed for 13 TeV as compared to 5.02 TeV and this might be understood as being due to the contributions from the hard scatterings in pp at $\sqrt{s} = 13$ TeV being higher as compared to 5.02 TeV.
- Similar behavior for the Tsallis temperature, T has been observed, which shows a significant dependence on the multiplicity classes. A correlation between T and q is clearly observed.
- Comprehensive study of the extracted parameters dependence on the fitting range of charged particle transverse momentum spectra is performed for the highest and lowest charged particle multiplicity classes for both the energies.
- The non-extensive parameter, q shows a reverse trend for both highest and lowest multiplicity classes as a function of fitting range.
- For the V0M1 class (corresponds to highest multiplicity), the addition of the high- p_T charged particles increases the power-law contributions, which leads to the lower values of q with extending the fitting range in the non-extensive statistics. On the other hand, for the V0M10 class (corresponds to the lowest multiplicity), extending the fitting range has less power-law contribution (as compared to V0M1). The q values for V0M10 show an increase with the fitting range in the non-extensive statistics.
- $p_T \sim 8$ GeV/c, which shows a saturation behavior in T , q and χ^2/ndf seems to be a threshold for a different behavior in particle production. This needs a closure look.

- Similarly, Tsallis temperature, T evolves with fitting range and has opposite behavior for both V0M1 and V0M10 classes. The Tsallis temperature, T increases with fitting range for V0M1 class, whereas the trend for V0M10 class is reverse with the fitting range.

- Furthermore, the bulk part (up to $\simeq 2.5$ GeV/c) of the transverse momentum spectra of the charged particle has been characterized using BGBW model and extracted the transverse collective flow velocity ($\langle \beta \rangle$) and the kinetic freeze-out temperature (T_{kin}) as a function of charged particle multiplicity.

- The collective radial flow velocity, $\langle \beta \rangle$ is almost independent of the collision energy and multiplicity classes. The kinetic freeze-out temperature, T_{kin} however, shows a clear dependence on the multiplicity classes.

Conclusively, the BGBW explains the bulk part of the transverse momentum spectra and the description is better for the higher multiplicity classes, whereas the non-extensive Tsallis statistics describes the charged particle transverse momentum for the complete p_T -range for all the multiplicity classes and collision energies. The latter observation is expected as the dominant high- p_T contribution comes from jet fragmentation and are described by pQCD processes, which show up in the power-law tail of the spectra.

Acknowledgment

The authors acknowledge the financial supports from ALICE Project No. SR/MF/PS-01/2014-IITI(G) of Department of Science & Technology, Government of India. RR acknowledges the financial support by DST-INSPIRE program of Government of India.

-
- [1] J. Adam *et al.* [ALICE Collaboration], *Nature Phys.* **13**, 535 (2017).
- [2] J. Cleymans and D. Worku, *J. Phys.* **G 39**, 025006 (2012).
- [3] J. Cleymans and D. Worku, *Eur. Phys. J. A* **48**, 160 (2012).
- [4] J. Cleymans, G. I. Lykasov, A. S. Parvan, A. S. Sorin, O. V. Teryaev, D. Worku, *Phys. Lett.* **B 723** 351 (2013).
- [5] M. D. Azmi, J. Cleymans, *J. Phys.* **G 41**, 065001 (2014).
- [6] C. Y. Wong and G. Wilk, *Phys. Rev.* **D 87**, 114007 (2013).
- [7] C. Y. Wong, G. Wilk, L. J. L. Cirlo, C. Tsallis, arXiv:1412.047 [hep-ph].
- [8] G. Wilk, Z. Włodarczyk, *Physics* **A 413**, 53 (2014).
- [9] G. Wilk, Z. Włodarczyk, arXiv: 1403.3508[hep-ph].
- [10] K. Urmosy, G. G. Barnaföldi, S. Harangozó, T. S. Biró and Z. Xu, arXiv:1501.02352 [hep-ph].
- [11] A. Khuntia, H. Sharma, S. Kumar Tiwari, R. Sahoo and J. Cleymans, *Eur. Phys. J. A* **55**, 3 (2019).
- [12] A. Khuntia, S. Tripathy, R. Sahoo and J. Cleymans, *Eur. Phys. J. A* **53**, 103 (2017).
- [13] L. J. L. Cirlo, C. Tsallis, C. Y. Wong, G. Wilk, arXiv:1409.3278 [hep-ph].
- [14] C. Tsallis, *J. Stat. Phys.* **52**, 479 (1988).
- [15] T. Bhattacharyya, J. Cleymans, A. Khuntia, P. Pareek and R. Sahoo, *Eur. Phys. J. A* **52**, 30 (2016).

- [16] T. Bhattacharyya, P. Garg, R. Sahoo and P. Samantray, *Eur. Phys. J. A* **52**, 283 (2016).
- [17] G. Wilk and Z. Włodarczyk, *Phys. Rev. Lett.* **84**, 2770 (2000).
- [18] S. Acharya *et al.* [ALICE Collaboration], arXiv:1905.07208 [nucl-ex].
- [19] M. Rybczynski, Z. Włodarczyk, *Eur. Phys. J. C* **74**, 2785 (2014).
- [20] E. Schnedermann, J. Sollfrank and U. W. Heinz, *Phys. Rev. C* **48**, 2462 (1993).
- [21] J. D. Bjorken, *Phys. Rev. D* **27**, 140 (1983).
- [22] P. Huovinen, P. F. Kolb, U. W. Heinz, P. V. Ruuskanen and S. A. Voloshin, *Phys. Lett. B* **503**, 58 (2001).
- [23] Z. Tang *et al.*, *Chin. Phys. Lett.* **30**, 031201 (2013).
- [24] D. Thakur, S. De, R. Sahoo and S. Dansana, *Phys. Rev. D* **97**, 094002 (2018).
- [25] N. Sharma, J. Cleymans, B. Hippolyte and M. Paradza, *Phys. Rev. C* **99**, 044914 (2019).